THE JOURNAL OF PHYSICAL CHEMISTRY C

Article

pubs.acs.org/JPCC

Poly(*o*-toluidine) Nanowires Based Organic Field Effect Transistors: A Study on Influence of Anionic Size of Dopants and SWNTs as a Dopant

Prasanta Ghosh,[†,⊥] Kunal Datta,[†,⊥] Ashok Mulchandani,[‡] Sung-Hwan Han,[§] Pankaj Koinkar,[∥] and Mahendra D. Shirsat*[,†]

[†]Intelligent Materials Research Laboratory, Department of Physics, Dr. Babasaheb Ambedkar Marathwada University, Aurangabad (MS), 431004, India

[‡]Department of Chemical and Environmental Engineering, University of California, Riverside, Riverside, California 92507, United States

[§]Department of Chemistry, Hanyang University, Seoul, South Korea

[∥]Center for International Cooperation in Engineering Education, University of Tokushima, Tokushima, Japan

ABSTRACT: Poly(*o*-toluidine) [P(OT)] nanowires electrode junction based organic field effect transistors (OFETs) with back-gated architecture are demonstrated. P(OT) nanowires have been site specifically synthesized to bridge Au micropatterns on Si/SiO_2 substrate by facile galvanostatic route. Dopants with various sizes of anions have been employed during electrochemical synthesis of nanowires to study the possible impact of the same on electrochemical, morphological, spectroscopic, electrical, and FET characteristics. Observations show that varying the size of dopants significantly modulates crucial characteristic features of the FETs especially charge carrier mobility (μ) and on−off ratio (I_{on}/I_{off}). A probable model of the observed behavior suggests the anionic size of the dopants to be a dominant factor in deciding the conduction behavior of the FETs, and such rationalization is supported by spectroscopic and electrical data obtained. The device fabricated with carboxylated SWNTs as dopant exhibited superior FET properties than its counterparts in terms of $\mu = 3.17 \times 10^{-4}$ cm^2 V^{-1} s^{-1} and $I_{on}/I_{off} = 1.85 \times 10^4$.

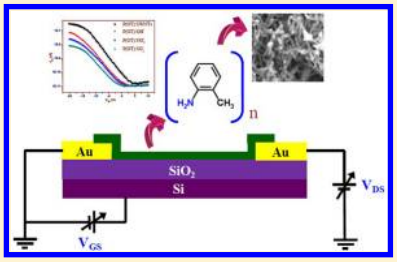

INTRODUCTION

Present research impetus on one-dimensional (1-D) nanostructures is critically driven by the necessity for minimizing feature dimensions in order to achieve higher degree of operational efficiency, material flexibility, device integration, and footprint minimization. Among pronounced 1-D nanomaterials, carbon nanotubes (CNTs) and nanowires of conducting polymers (CP)/metal oxides/silicon, etc., have received substantial attention in the field of miniaturized electronics,[1−4] chemical and biological sensing,[5−7] and photovoltaics.[8−10] CP nanowires, however, has remained at the center of interest for a large spectrum of research efforts since polymers exhibit unparallel flexibility in processing capabilities along with appealing electrical, magnetic, and optical properties of metals and/or semiconductors.[11,12] Rather importantly, electrical conductivity of CP materials can be easily modulated by oxidative and reductive doping,[13] a classic property that has always put these materials a step ahead of their counterparts. At the same time, electrochemical synthesis offers a facile route to synthesize CP nanowires with excellent site specificity.[14,15] Such attractive properties, amalgamated with present stature of microfabrication technology, have revolutionized the concepts of traditional (inorganic) semiconductor devices and organic field effect transistors (OFETs) based on polymeric materials stand as a prominent representative of this all emerging change.

The performance of OFETs is generally denoted by several characteristic parameters that include carrier mobility (μ), on/off ratio (I_{on}/I_{off}), and threshold voltage (V_{TH}). Carrier mobility defines the ease with which the charge carriers can move through the channel when a drain to source bias is applied while switching characteristics of an FET is illustrated by the on/off current ratio of the device. For applications ranging from complex chemical sensing platforms to simple large area electronics, fast and efficient charge movement and clear switching behavior are general prerequisites. Hence, these sectors are of vital interest where continuous improvements are necessary. In order to obtain such betterments, (i) controlling the morphology, chemical modifications, and molecular alignment of the active layer,[16−18] (ii) modulation in the device architecture,[19] and (iii) engineering of the gate dielectric material[20,21] are reported to yield encouraging outcomes, yet active layers have succeeded to attract maximum attention. Several OFETs with polymeric materials have been achieved with mobility more than 1 cm^2 V^{-1} s^{-1},[22,23] in comparison to the present state of amorphous silicon (where mobility typically ranges from 0.1 to 1 cm^2 V^{-1} s^{-1}). Derivatives of polythiophene[22−25] are among the highest reported CPs as

Received: May 12, 2013
Revised: July 2, 2013

   dx.doi.org/10.1021/jp404674j | *J. Phys. Chem. C* XXXX, XXX, XXX−XXX

active layers of OFETs. However, in most of the reported cases, the active material is in the form of polymeric thin films. FET structure with CP nanowires as active materials has found very little interest till date, especially from the perspective of investigation toward optimization of device performance. At the same time, consistent demands for betterment ask for the study of varied range of polymers.

The present investigation deals with facile electrochemical templateless synthesis of conducting polymer nanowires on electrode junctions (CPNEJs)[14] of poly(*o*-toluidine) [P(OT)] bridging a 3 μm gap between two lithographically patterned Au electrodes on a conventional Si/SiO_2 substrate that finally served as active material for a back-gated FET structure. This technique was first demonstrated by Alam et al.[14] for fabrication of CP nanowires based electrolyte gated FET structures. In spite of the simplicity and control over the dimension of nanowires offered by this technique, not much interest was found to be evinced in this direction in later course of work on OFETs. The P(OT) nanowires based back-gated FETs fabricated in the present investigation, to the best of our knowledge, is the first of its type, and the report embodies initial findings of the work being carried by us toward development of back-gated OFETs with polymeric 1-D structures as active material. P(OT) is perhaps the most widely explored derivative of poly(aniline) that possesses excellent processabilty as well as good thermal and environmental stability.[26] Reports have demonstrated interesting outcomes with P(OT)/metal contact Schottkey diodes.[27,28] In the present work, the authors have probed the role of anionic radii of employed dopants in tuning the FET characteristic parameters. Although several literatures[29,30] have discussed the effects of dopant type on polymeric properties, the specific aspect of anionic size of dopants is not well explored. Dopants that were employed during on site synthesis of the P(OT) nanowires are listed as follows in ascending order of anionic radii: potassium hydroxide (OH^- ~ 133 pm) < sodium nitrate (NO_3^- ~ 179 pm) < sulfuric acid (SO_4^- ~ 258 pm)[31] ≪ SWNT. Attempting SWNTs as dopants is certainly an offbeat attempt. As a matter of fact, carboxylated SWNTS (COOH-SWNTs) have been reported to act as anionic dopants,[32,33] and the present study aims toward investigating possible effects of the same in FET performance in contrast to conventional dopants.

EXPERIMENTAL SECTION

Fabrication of OFETs. Heavily doped Si (P^+) substrate with a 300 nm thermal oxide layer served as the platform for OFETs. The Au source and drain electrodes having a separation of 3 μm were structured on the Si/SiO_2 wafer by transferring micropatterns through photomasks followed by subsequent deposition of 20 nm Cr adhesive layer and 180 nm Au layer by e-beam evaporation and thermal evaporation, respectively. The syntheses of P(OT) nanowires were carried out in a typical three-electrode configuration. The source and drain electrodes were wire bonded [West Bond; 7476D] and externally shorted to form the working electrode. A Pt wire [CH Instruments; CHI115] and an Ag/AgCl wire (chlorinated Ag wire) served as counter and quasi-reference electrode,[34] respectively. Effective surface area of the working electrodes was reduced by stamping of epoxy glue.[5] From optical microscopy image, the effective surface area was determined to be ca. 38 854 μm^2.

Typically, the electrolyte solution employed for polymerization consisted of monomer (*o*-toluidine; >99%; Sigma-Aldrich; as received) and dopants (H_2SO_4, KOH, and KNO_3; Rankem/India) at respective concentrations of 0.25 and 0.15 mM in water. In another attempt, COOH-SWNTS (Nanoshell Inc., Wilmington, DE) were ultrasonically dispersed in water (0.01 mg mL^{-1}) for 2 h followed by addition of *o*-toluidine (0.25 M) and was kept under continuous stirring for 24 h at room temperature. All electrolytes were synthesized in HPLC grade water (RANKEM, India) and deoxygenated prior to synthesis. For electrochemical bridging of the source and drain electrode, a 0.5 μL of the electrolytes were placed on the target Au micropatterns. A single-step galvanostatic route was employed for electrolyte containing SWNTs, and for the rest of the cases, typical two-step deposition[35] were carried out. The reference and counter electrodes were attached to precision micropositioners to ensure accurate contact with the electrolyte. An anodic current density of 0.5 $mA/cm^2$was impressed on the working electrode for 900 s for the single-step deposition. The two-step deposition was carried out by initially applying an anodic current density of 0.05 mA/cm^2 (1200 s) followed by lowering the current density to 0.02 mA/cm^2 (5400 s). The electrochemical deposition were carried out by a electrochemical workstation (CH Instruments; CHI 660C)

Characterization Techniques. Field emission scanning electron microscopy (FESEM) images were recorded (FESEM; Hitachi S4800) to examine the surface morphology of fabricated devices. *I*−*V* characteristics were recorded by linearly sweeping potential from −1 to +1 V (CHI660C). Spectroscopic studies were carried out by a UV−vis spectrophotometer (UV 2450, Shimadzu). Field effect transistor (FET) characteristics (forward and transfer) in back-gated configuration were recorded with a Keithley 2636 A dual channel source measure unit. For studying the forward characteristics, drain to source voltage (VDS) was swept from 0 to −25 V while varying the gate to source voltage (VGS). Transfer characteristics were obtained by sweeping the VGS from −20 to +20 V at fixed VDS (−10 V). The *I*−*V* and FET measurements were recorded under ambient conditions. For estimating the stability of the best observed FET platform, i.e., SWNTs doped P(OT) nanowires, mobility of a particular device was estimated every 5 days by recording transfer characteristics as described above. The investigation was carried for 150 days.

RESULTS AND DISCUSSION

Electrochemical and Morphological Studies. Figure 1 shows the chronopotentiogram recorded during electrodeposition for P(OT) nanowires under different dopant conditions. During two-step galvanostatic synthesis, the effective potential for various dopants at the working electrode was found to lie in the range of 0.42−0.37 V during the first step and observed to be decreased to the range of 0.38−0.36 V during the final step. Typically, the first step of a two-step galvanostatic process initiates the nucleation of polymeric seeds on the electrode surface while during the subsequent step, growth of the nanowires occur from the nucleation sites.[35] The chronopotentiogram for single-step galvanostatic deposition of P(OT) nanowires with SWNTs as dopants is given as inset of Figure 1. A single-step deposition was employed in this case since the SWNTs are supposed to act as nucleation sites for the polymer owing to their highly conductive surface. Hence, initial nucleation step that was required for other dopants needed not to be employed. The polymerization potential for P(OT)/

dx.doi.org/10.1021/jp404674j | J. Phys. Chem. C XXXX, XXX, XXX−XXX

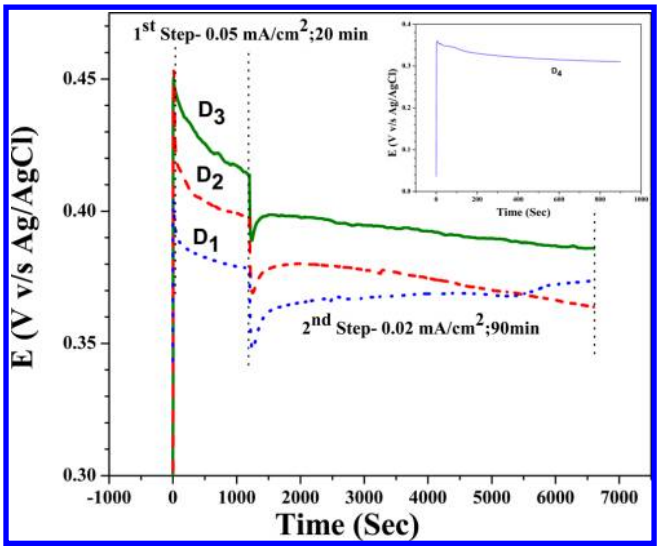

Figure 1. Chronopotentiograms for two-step galvanostatic synthesis of P(OT) nanowires with various dopants. Inset: chronopotentiogram for P(OT)/SWNT nanowires synthesis by single-step deposition.

SWNTs (D_4; as denoted hereafter) was recorded to be the lowest (0.31 V). The polymerization potential for other devices were found to follow the order P(OT)/KOH (D_1) < P(OT)/KNO_3 (D_2) < P(OT)/H_2SO_4 (D_3). A lower polymerization potential is indicative toward higher electrical conductivity of the yield.[36]

Typical FESEM image of P(OT) nanowires (with KOH as dopant) along with the optical microscope image of the Au fingertips is given in Figure 2. The FESEM image shows formation of uniform dendritic P(OT) nanowires with

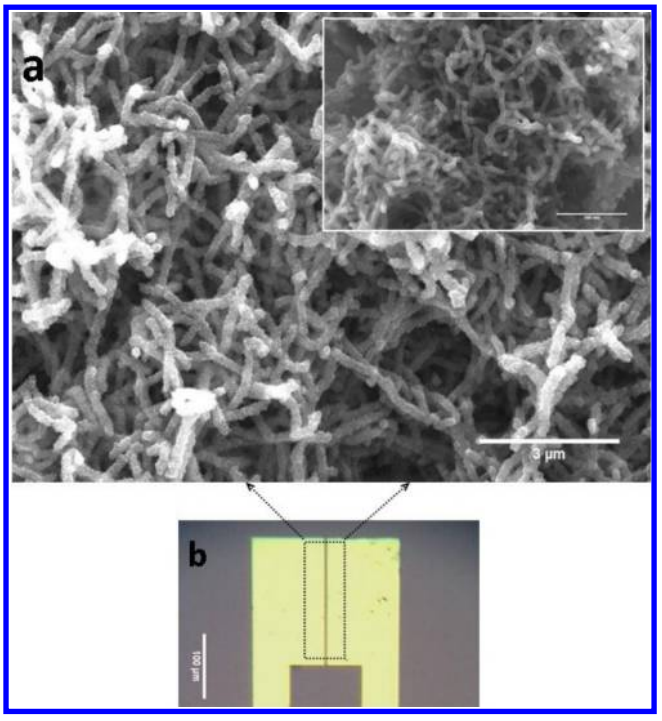

Figure 2. (a) FESEM image of P(OT) nanowires (KOH as dopant). Inset: FESEM of P(OT)/SWNT device. (b) Optical microscope image of the Au micropattern (3 μm apart) that served as source-drain electrodes.

numerous intertwines. The average diametric distribution of the nanowires was found to lie within 200−250 nm. Similar morphological nature could be observed in case of other devices (i.e., D_2 and D_3; data not shown).

This is a striking difference with the thin film modality of polymers where dopants are reported to have considerable impact on morphological features.[28,29,37] Thus, the applied current density of the initial step of the two-step galvanostatic synthesis seems to be the prime deciding factor for the diameter of synthesized nanowires. Inset of Figure 2 shows the FESEM image of the P(OT) nanowires (average diameter 30−40 nm) synthesized with SWNTs as dopant. A steep decrease in the average diameter of the nanowires in this case certainly ensures that the SWNTs have acted as nucleation sites for polymeric growth.

Electronic Spectroscopy Studies. Figure 3 represents the UV spectra of P(OT) nanowires synthesized with various

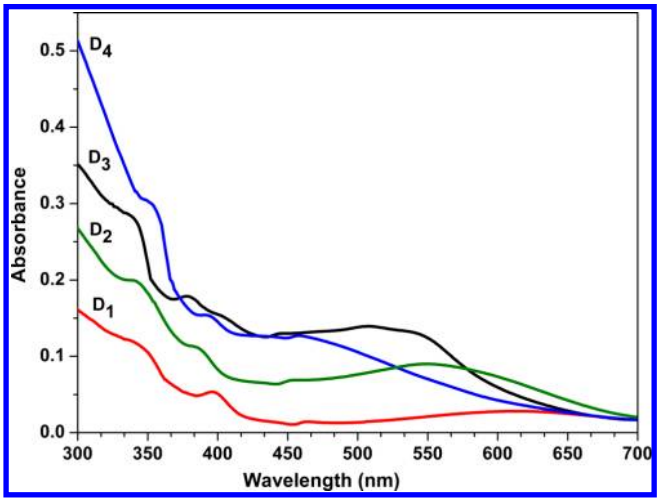

Figure 3. UV−vis spectra of P(OT) nanowires with various dopants.

dopants. The spectra reveals well-defined absorptions around 345 nm signifying $\pi-\pi^*$ transitions in benzene rings. The absorptions near 385 nm represents the polaron generation, suggesting the occurrence of bipolaronic transitions. The humps around 460 nm are assigned to n−π^* transitions between HOMO orbital of the benzenoid ring and LUMO orbital of the quinoid ring. The broad 550 nm band is often assigned to the polaronic transitions. The observations are well in line with earlier reported literature.[28,38−40] As evidenced from the spectra, the P(OT)/SWNT device has exhibited the characteristic peaks with greater intensity than others, demonstrating well-defined π-electron resonance.[41] The band gap determined for the $\pi-\pi^*$ transitions corresponding to the first absorption band were calculated using the formula $\Delta E = hc/\lambda_{\pi-\pi^*}$ ($h = 6.625 \times 10^{-34}$ J s and $c = 3 \times 10^8$ ms^{-1})[29] and given in Table 1. The band gap values were found to lie in the order $D_1 < D_2 < D_3$ corresponding to the hypsochromic shift in $\pi-\pi^*$ transition wavelength in accordance with the increase in ionic radii for all dopants when SWNTs stood as the exception, empirically, for the reason already defined.

Electrical and FET Measurements. Apart from the P(OT)/SWNTs device, all other devices revealed linearity and symmetry in current/voltage relation as shown in Figure 4. Thus, formation of the ohmic contacts indicates lower work function of the synthesized polymeric matrices than Au (ϕ_{Au} = 5.1 eV).[27,42] However, for the P(OT)/SWNTs device,

dx.doi.org/10.1021/jp404674j | J. Phys. Chem. C XXXX, XXX, XXX−XXX

Table 1. Band Gap Values Synthesized P(OT) Nanowires with Various Dopants and Resistance of Corresponding Devices

device	band gap (eV)	resistance (MΩ)
D_1	3.61	11.04
D_2	3.63	12.20
D_3	3.66	15.60
D_4	3.50	3.80

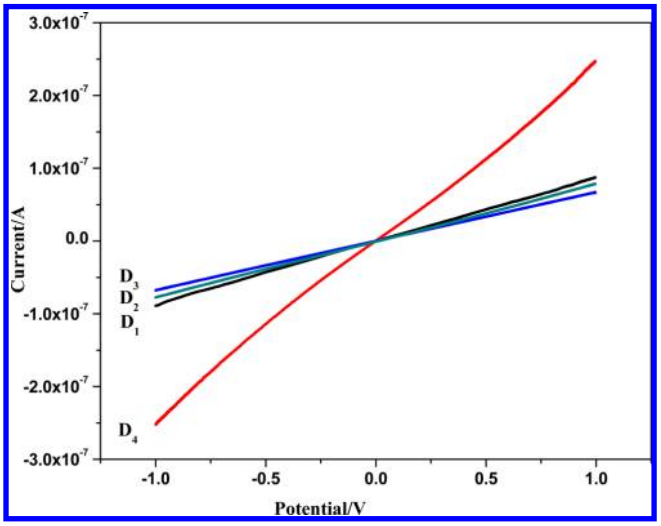

Figure 4. Room temperature I/V characteristics of P(OT) nanowires with various dopants.

nonlinearity could be observed that can probably be attributed to the formation of slightly rectifying contacts due to the presence of semiconducting SWNTs with small band gap.[43] Device resistance was determined by calculating inverse of the slope of current−voltage curves for the linear devices. For the P(OT)/SWNTs device, the absolute linear portion current voltage characteristic (for a potential window of 0.3 V with centered null current) was considered for calculation of the device resistance. The resistance values have been presented in Table 1. The best observed conduction behavior for the P(OT)/SWNTs can be attributed to efficient coupling between P(OT) and SWNTs leading to overlap of wave functions and enhancement in average localization length.[44] The device resistance values are found to be in sound agreement to the band gap values.

The FET characteristics of the P(OT) nanowires devices with different dopants are given in Figures 5 and 6. As depicted by the typical output characteristics (Figure 5a−d), all the devices have exhibited p-type nature with well-defined linear and saturation behavior that conforms well to conventional FET models in both the regimes of operation. The maximum saturation current was recorded for D_4 while the rest of the devices followed the order $D_1 > D_2 > D_3$. At the same time, it can be well observed that the pinch-off voltage (V_p) for the fabricated devices is strongly dependent on the anionic size of dopants. Dopants with higher anionic radii were observed to exhibit lower V_p in regularized manner with SWNTs based device (D_4), again, as exception. The control on V_p allows to tune the width of the saturation region and enables to lower the operating V_{DS} of the devices.

Figure 6 gives the transfer characteristics of the fabricated devices recorded at constant V_{DS} (−10) V. All the fabricated devices have exhibited off state current in the order of 10^{-11}A that is significantly lower than earlier reported electrolyte gated FETs[14] or single nanowires based FETs.[3] Measurably higher off sate current for D_4, in contrast to other devices, could probably be attributed to the presence of metallic SWNTs. The devices could also be characterized with excellent switching behavior. Highest I_{on}/I_{off} factor could be recorded for D_4 (1.85×10^4) that is comparable to reported pentacene-SWNTs based TFTs.[45] The charge carrier mobilities and I_{on}/I_{off} of all the investigated devices have been estimated from the transfer curves, and the average and maximum values of the same are furnished in Figure 7. Device transconductance ($g_m = dI/dV_g$) were estimated in linear regime to determine charge carrier mobility values by the formula $\mu = L^2_{SD}g_m/C_GV_{DS}$.[2] For these analyses, full parallel plate gate capacitance $C_G = \varepsilon WL_{SD}/L_{OX}$ (W = 200 μm, L_{SD} = 3 μm, L_{OX} = 300 nm) was used. The regularity in the trends in carrier mobility and I_{on}/I_{off} values is in inclination with the fact that higher carrier mobility leads to high on current values that ultimately contributes to a higher I_{on}/I_{off} factor.[46] Apart from SWNTs, we could observe an orderly shift in the threshold voltage (V_{TH}) toward more positive value when the anionic radius of dopant is decreased. Most importantly, very low device to device performance variation could be observed in all cases. Thus, the questionable effects of intertwines of nanowires on device performance (that can be mitigated with aligned/single nanowires) can well be traded off with the ease of fabrication of the present modality of device active layer.

Conduction behavior in a polymeric material is known to be dependent on the movement of charge carriers along a chain (intrachain hopping) and across the chain (interchain hopping). Such conduction is bound to be highly affected by the pinning of charge carriers to their dopant counterions by electrostatic attraction. This situation can be further elucidated as self-trapping of charge by the deformation it induces in the chain.[46] As a matter of fact, theoretical calculations suggest that in lightly doped semiconductors about 97% dopants form charge transfer complexes which hardly contribute to charge transport.[47] Thus, the situation can be envisaged as the formation of deep Coulomb wells filled with self-trapped charges introduced by dopants.[48] From this standpoint, perusal of the size of dopant anions leads to certain interesting conclusions. Electrostatics suggests that Coulombic attraction is higher for spherically symmetric charged particle with smaller radius which readily allows inferring that for anions with lower radius trapping of charge carriers is more severe. Thus, accumulated charges in polymeric FET structures are supposed to experience less electrostatic attraction for small anionic dopants as Coulomb wells are already filled with self-trapped charges induced by dopants.[48] Such situation results in large number of free charge carriers in the conduction backbone, and equally, conduction behavior is better in terms of better inter- and intrachain hopping. However, difficulty arises if larger sized dopants are considered since in such cases, charge carriers are less affected by electrostatic attraction. Hence, to rationalize the $I-V$ and FET data that show poor conduction/FET behavior for larger sized dopants, it may be hypothesized that since Coulombic wells are less filled in such cases, accumulated charge carriers are more susceptible to trapping. The trend that could be observed for V_{TH} values also supports this view since, more positive values of gate potential is needed to be applied to deplete the channel in case of higher mobile charge carrier density which is the case with lower sized dopants. Also, as the

dx.doi.org/10.1021/jp404674j | J. Phys. Chem. C XXXX, XXX, XXX−XXX

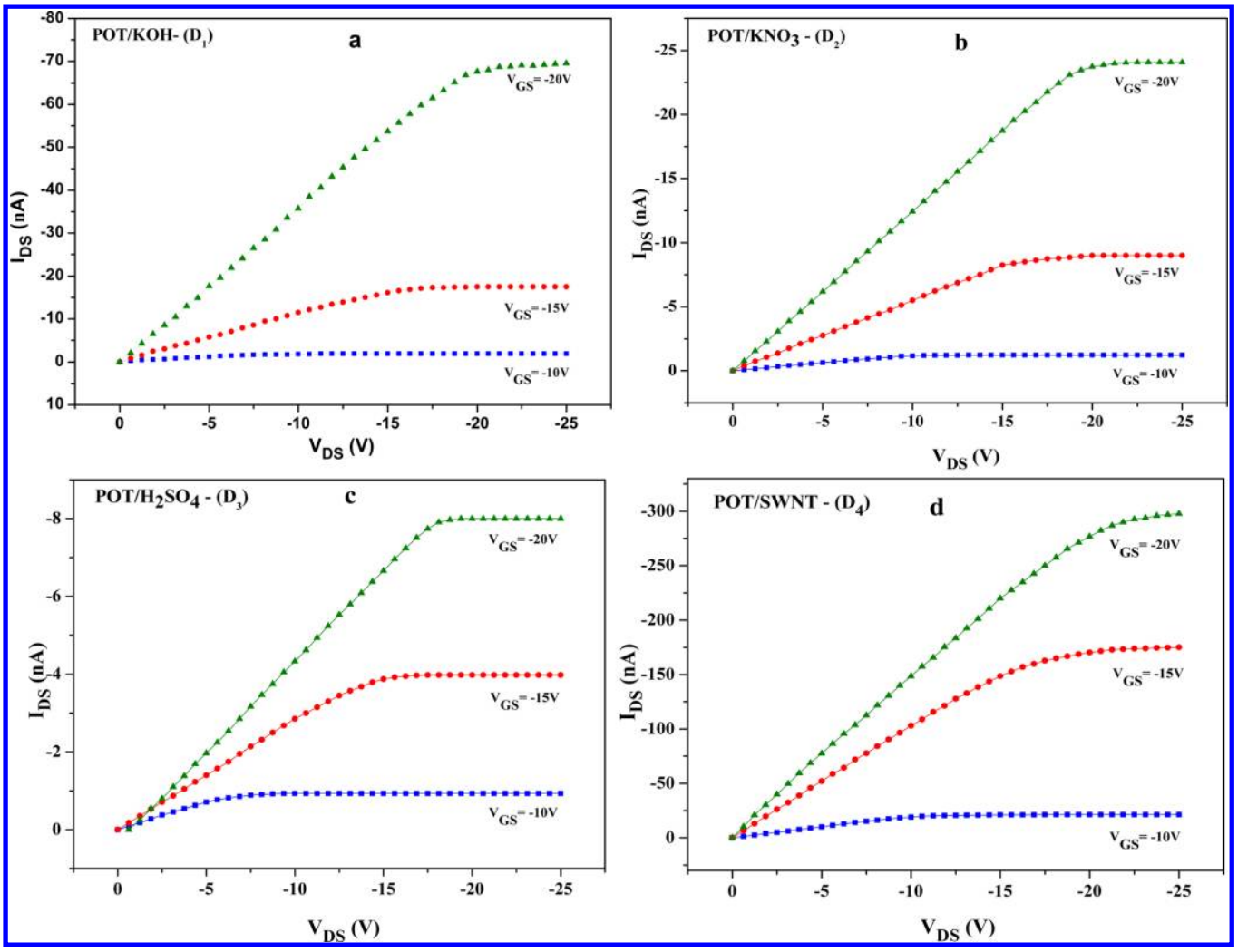

Figure 5. Output characteristics of (a) D_1, (b) D_2, (c) D_3, and (d) D_4 for different V_{GS} values.

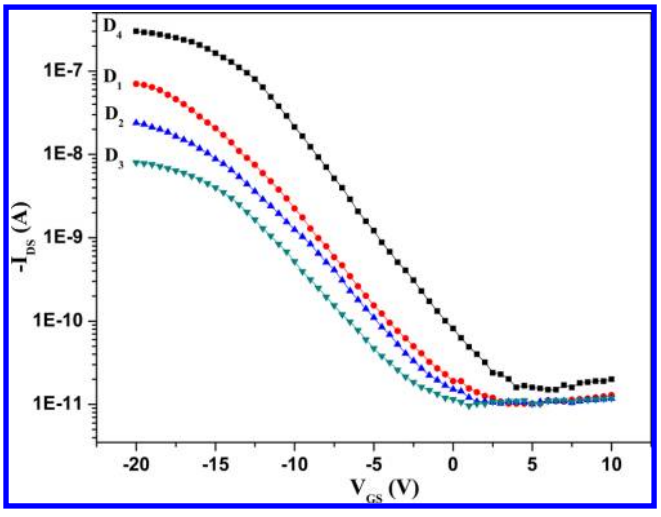

Figure 6. Transfer characteristics of the fabricated devices.

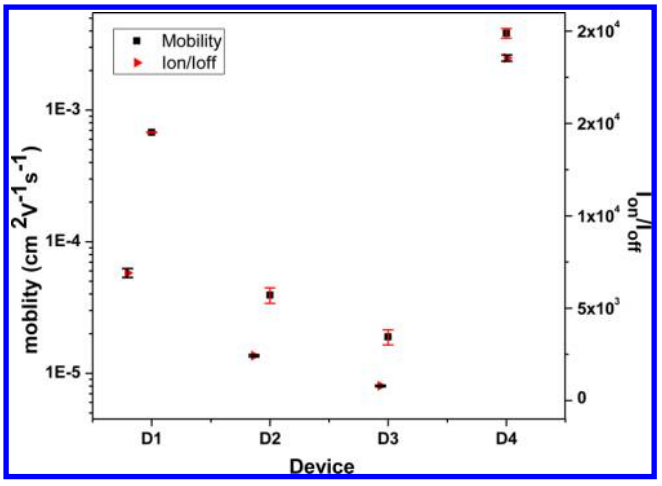

Figure 7. Mobility and on/off ratio of the fabricated devices (at least seven devices were tested in each case).

anionic size was increased, the lowering in crystallinity resulted in enhanced interchain separation, thereby hindering the interchain hopping component of the conduction mechanism.[29] The conduction behavior is well supported by the spectroscopic data that certainly indicates higher degree of conjugation in polymeric chain for small anionic dopants.

Although the above model of conduction behavior stands well for D_1, D_2, and D_3, the stiff exception that could be observed in case of D_4 may be attributed to the high π-electron resonance of SWNTs with P(OT) backbone as suggested by

dx.doi.org/10.1021/jp404674j | J. Phys. Chem. C XXXX, XXX, XXX−XXX

spectral and $I-V$ data. In this particular case, the extent of delocalization of the charge carriers with π-electron cloud probably accounts for the superior conduction behavior than other devices. At the same time, lower cross section of SWNTs doped P(OT) nanowires results in reduction of phase space for scattering, thereby enhancing the bulk mobility along the nanowires structure.[49] Finally, the highest value of V_{TH} observed for this devices, could possibly be ascribed to the presence of higher carrier density at the interfacial layer of P(OT)/SWNTs. We are presently exploring the fabricated FET devices for possible gas sensing applications.

Stability of the Best FET Platform. A very negligible drift could be observed (Figure 8) in the performance of the device

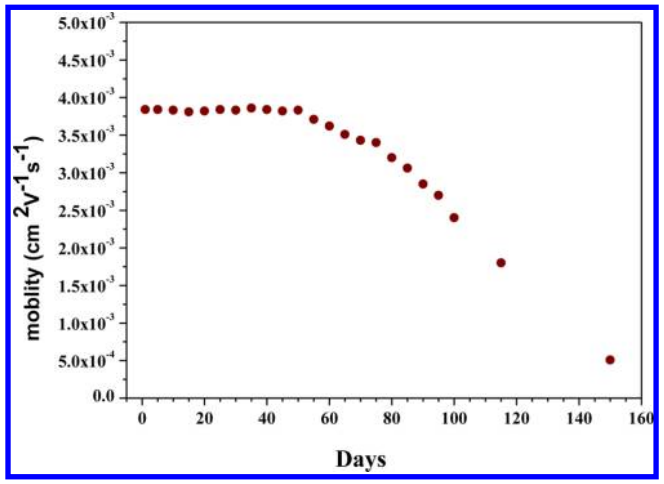

Figure 8. Stability characteristics of the FET platform.

until 70 days with a maximum deviation of 10.67% from the initial value of mobility. Rapid fall in the FET performance thereafter could well be attributed to the natural degradation of polymer.

CONCLUSION

In summary, OFETs containing P(OT) nanowires as active semiconductor layer were fabricated. Two-step galvanostatic deposition proved to be a facile route for synthesis of nanowires electrode junctions on Si/SiO_2 substrate. Dopants with various anionic radii were employed during electrochemical synthesis. Apart from SWNTs, anionic size was not found to affect the morphological features of synthesized nanowires. Steep decrease in average diameter of nanowires with SWNTs as dopants suggests the role of SWNTs as templates for polymerization. UV–vis spectroscopic studies have shown that dopants with smaller anionic size offer higher degree of conjugation in polymeric chain that is responsible in shaping the conduction characteristics of the material. The $I-V$ and FET observations were correlated in terms of variation in electrostatic attraction and trapping offered by dopants with different anionic size. All the fabricated devices have exhibited p-type conduction while retaining basic FET characteristics. Crucial FET parameters, viz., V_p, V_{TH}, μ, and I_{on}/I_{off} are found to be easily modulated by changing anionic size of dopants and observations show sheer regularity for dopants KOH, KNO_3, and H_2SO_4. An interesting direction of further investigation can be toward pursuit of a trivial point where requisite device V_p and corresponding mobility can be achieved for low power application by varying dopant dimension. The exceptional behavior of the device with SWNTs as dopant could be attributed to high π-electron resonance of SWNTs with P(OT) backbone.

AUTHOR INFORMATION

Corresponding Author

*E-mail: mds_bamu@yahoo.co.in, mdshirsat@gmail.com (M.D.S.).

Author Contributions

$^{\perp}$P.G. and K.D. contributed equally.

Notes

The authors declare no competing financial interest.

ACKNOWLEDGMENTS

P.G., K.D., and M.D.S. are thankful for financial assistance to Department of Science and Technology (DST), Nanomission, New Delhi, India (Grant SR/NM/NS-94/2009), Department of Science and Technology (DST), TSD, New Delhi, India (Grant DST/TSG/PT/2010/11-C & G), and Inter University Accelerator Centre (IUAC), New Delhi, India (Grant IUAC/XIII.7/UFR-48309/984).

REFERENCES

(1) Martel, R.; Schmidt, T.; Shea, H. R.; Hertel, T.; Avouris, P. Single- and Multi-Wall Carbon Nanotube Field-Effect Transistors. *Appl. Phys. Lett.* **1998**, *73*, 2447–2449.

(2) Snow, E. S.; Campbell, P. M.; Ancona, M. G.; Novak, J. P. High-Mobility Carbon-Nanotube Thin-Film Transistors on a Polymeric Substrate. *Appl. Phys. Lett.* **2005**, *86* (033105), 1–3.

(3) Wanekaya, A. K.; Bangar, M. A.; Yun, M.; Chen, W.; Myung, N. V.; Mulchandani, A. Field-Effect Transistors Based on Single Nanowires of Conducting Polymers. *J. Phys. Chem. C* **2007**, *111*, 5218–5221.

(4) Cui, Y.; Zhong, Z.; Wang, D.; Wang, W. U.; Lieber, C. M. High Performance Silicon Nanowire Field Effect Transistors. *Nano Lett.* **2003**, *3*, 149–152.

(5) Wang, Y.; Coti, K. K.; Wang, J.; Alam, M. M.; Shyue, J. J.; Lu, W.; Padture, N. Individually Addressable Crystalline Conducting Polymer Nanowires in a Microelectrode Sensor Array. *Nanotechnology* **2007**, *18* (424021), 1–7.

(6) Ramanathan, K.; Bangar, M. A.; Yun, M.; Chen, W.; Myung, N. V.; Mulchandani, A. Bioaffinity Sensing Using Biologically Functionalized Conducting-Polymer Nanowire. *J. Am. Chem. Soc.* **2005**, *127*, 496–497.

(7) Huang, J.; Wan, Q. Gas Sensors Based on Semiconducting Metal Oxide One-Dimensional Nanostructures. *Sensors* **2009**, *9*, 9903–9924.

(8) Liu, K.; Qu, S.; Zhang, X.; Tan, F.; Wang, Z. Improved Photovoltaic Performance of Silicon Nanowire/Organic Hybrid Solar Cells by Incorporating Silver Nanoparticles. *Nanoscale Res. Lett.* **2013**, *8* (88), 1–6.

(9) Bindl, D. J.; Arnold, M. S. Semiconducting Carbon Nanotube Photovoltaic Photodetectors. *Int. J. High Speed Electron. Syst.* **2011**, *20*, 687–695.

(10) Fu, K.; Sun, C.; Mathews, N.; Mhaisalkar, G. S. Dye-Sensitized Solar Cells Based on Tin Oxide Nanowire Networks. *Nanosci. Nanotechnol. Lett.* **2012**, *4*, 733–737.

(11) Macdiarmaid, A. G. Synthetic Metals: A Novel Role for Organic Polymers (Nobel Lecture). *Angew. Chem., Int. Ed.* **2001**, *40*, 2581–2590.

(12) Heeger, A. J. Semiconducting and Metallic Polymers: The Fourth Generation of Polymeric Materials (Nobel Lecture). *Angew. Chem., Int. Ed.* **2001**, *40*, 2591–2611.

(13) Janata, J.; Josowicz, M. Conducting Polymers in Electronic Chemical Sensors. *Nat. Mater.* **2003**, *2*, 19–24.

(14) Alam, M. M.; Wang, J.; Guo, Y.; Lee, S. P.; Tseng, H. R. Electrolyte-Gated Transistors Based on Conducting Polymer Nanowire Junction Arrays. *J. Phys. Chem. B* **2005**, *109*, 12777−12784.
(15) Wang, J.; Chan, S.; Carlson, R. R.; Luo, Y.; Ge, G.; Ries, R. S.; Heath, J. R.; Tseng, H. R. Electrochemically Fabricated Polyaniline Nanoframework Electrode Junctions that Function as Resistive Sensors. *Nano Lett.* **2004**, *4*, 1693−1697.
(16) Briseno, A. L.; Mannsfeld, S. C. B.; Lu, X.; Xiong, Y.; Jenekhe, S. A.; Bao, Z.; Xia, Y. Fabrication of Field-Effect Transistors from Hexathiapentacene Single-Crystal Nanowires. *Nano Lett.* **2007**, *7*, 668−675.
(17) Park, Y. D.; Lim, J. H.; Jang, Y.; Hwang, M.; Lee, H. S.; Lee, D. H.; Lee, H. L.; Baek, J. B.; Cho, K. Enhancement of the Field-Effect Mobility of Poly(3-Hexylthiophene)/Functionalized Carbon Nanotube Hybrid Transistors. *Org. Electron.* **2008**, *9*, 317−322.
(18) Park, Y. D.; Kim, D. H.; Lim, J. A.; Cho, J. H.; Jang, Y.; Lee, W. H.; Park, J. H.; Cho, K. Enhancement of Field-Effect Mobility and Stability of Poly(3-hexylthiophene) Field-Effect Transistors by Conformational Change. *J. Phys. Chem. C* **2008**, *112*, 1705−1710.
(19) Liu, J.; Herlogsson, L.; Sawatdee, A.; Favia, P.; Sandberg, M.; Crispin, X.; Engguist, I.; Berggreen, M. Vertical Polyelectrolyte-Gated Organic Field-Effect Transistors. *Appl. Phys. Lett.* **2010**, *97* (103303), 1−3.
(20) Kelley, T. W.; Boardman, L. D.; Dunbar, T. D.; Muyres, D. V.; Pellerite, M. J.; Smith, T. P. High-Performance OTFTs Using Surface-Modified Alumina Dielectrics. *J. Phys. Chem. B* **2003**, *107*, 5877−5881.
(21) Singh, V. K.; Mazhari, B. Impact of Scaling of Dielectric Thickness on Mobility in Top-Contact Pentacene Organic Thin Film Transistors. *J. Appl. Phys.* **2012**, *111* (034905), 1−6.
(22) Tsao, H. N.; Cho, D. M.; Park, I.; Hansen, M. P.; Mavrinsky, A.; Yoon, D. Y.; Graf, R.; Pisula, W.; Spiess, H. W.; Mullen, K. Ultrahigh Mobility in Polymer Field-Effect Transistors by Design. *J. Am. Chem. Soc.* **2011**, *133*, 2605−2612.
(23) Tsao, H. N.; Cho, D.; Andreasen, J. W.; Rouhanipour, A.; Breibey, D. W.; Pisula, W.; Mullen, K. The Influence of Morphology on High-Performance Polymer Field-Effect Transistors. *Adv. Mater.* **2009**, *21*, 209−212.
(24) Lei, T.; Cao, Y.; Fan, Y.; Liu, C. J.; Yuan, S. C.; Pei, J. High-Performance Air-Stable Organic Field-Effect Transistors: Isoindigo-Based Conjugated Polymers. *J. Am. Chem. Soc.* **2011**, *133*, 6099−6101.
(25) Sirringhaus, H.; Tessler, N.; Thomas, D. S.; Brown, P. J.; Friend, R. H. High-Mobility Conjugated Polymer Field-Effect Transistors. *Adv. Solid State Phys.* **1999**, *39*, 101−110.
(26) Berrada, K.; Quillard, S.; Louam, G.; Lefrant, S. Polyanilines and Substituted Polyanilines: a Comparative Study of the Raman Spectra of Leucoemeraldine, Emeraldine and Pernigraniline. *Synth. Met.* **1995**, *69*, 201−204.
(27) Elmansouri, A.; Outzourhit, A.; Oueriagli, A.; Lachkar, A.; Hadik, N.; Achour, M. E.; Abouelaoualim, E.; Berrada; Ameziane, E. L. Spectroscopic Characterization of Electrodeposited Poly(o-toluidine) Thin Films and Electrical Properties of ITO/Poly(o-toluidine)/Aluminum Schottky Diodes. *Act. Passive Electron. Compon.* **2007**, *2007* (17846), 1−7.
(28) Elmansouri, A.; Outzourhit, A.; Lachkar, A.; Hadik, N.; Abouelaoualim, A.; Achour, M. E.; Oueriagli, A.; Ameziane, E. L. Influence of the Counter Ion on the Properties of Poly(O-Toluidine) Thin Films and Their Schottky Diodes. *Synth. Met.* **2009**, *159*, 292−297.
(29) Sinha, S.; Bhadra, S.; Khastgir, D. Effect of Dopant Type on the Properties of Polyaniline. *J. Appl. Polym. Sci.* **2009**, *112*, 3135−3140.
(30) Gade, V. K.; Shirale, D. J.; Gaikwad, P. D.; Kakde, K. P.; Savale, P. A.; Kharat, H. J.; Shirsat, M. D. Synthesis and Characterization of Ppy-PVS, Ppy-pTS, and Ppy-DBS Composite Films. *Int. J. Polym. Mater.* **2007**, *56*, 107−114.
(31) Jenkins, H. D. B.; Thakur, K. P. Reappraisal of Thermochemical Radii for Complex Ions. *J. Chem. Educ.* **1979**, *56*, 576.
(32) Zanello, L. P.; Zhao, B.; Hui, H.; Haddon, R. C. Bone Cell Proliferation on Carbon Nanotubes. *Nano Lett.* **2006**, *6*, 562−567.
(33) Ghosh, P.; Datta, K.; Mulchandani, A.; Sonkawade, R. G.; Asokan, K.; Shirsat, M. D. A Chemiresistive Sensor Based on Conducting Polymer/SWNT Composite Nanofibrillar Matrix-Effect of 100 Mev O^{16} Ion Irradiation on Gas Sensing Properties. *Smart Mater. Struct.* **2013**, *22* (035004), 1−8.
(34) Datta, K.; Ghosh, P.; More, M. A.; Shirsat, M. D.; Mulchandani, A. Controlled Functionalization of Single-Walled Carbon Nanotubes for Enhanced Ammonia Sensing: A Comparative Study. *J. Phys. D: Appl. Phys.* **2012**, *45* (355305), 1−8.
(35) Liang, L.; Liu, J.; Windisch, C. F., Jr.; Exarchos, G. J.; Lin, Y. Direct Assembly of Large Arrays of Oriented Conducting Polymer Nanowires. *Angew. Chem., Int. Ed.* **2002**, *41*, 3665−3668.
(36) Shirale, D. J.; Gade, V. K.; Gaikwad, P. D.; Kharat, H. J.; Kakde, K. P.; Savale, P. A.; Hussaini, S. S.; Dhumane, N. R.; Shirsat, M. D. The Influence of Electrochemical Process Parameters on the Conductivity of Poly(N-Methylpyrrole) Films by Galvanostatic Method. *Mater. Lett.* **2006**, *60*, 1407−1411.
(37) Riaz, U.; Ahmad, S.; Ashraf, S. M. Effect of Dopant on the Nanostructured Morphology of Poly(1-naphthylamine) Synthesized by Template Free Method. *Nanoscale Res. Lett.* **2008**, *3*, 45−48.
(38) Kumar, D. Poly(o-toluidine) Polymer as Electrochromic Material. *Eur. Polym. J.* **2001**, *37*, 1721−1725.
(39) Pron, A.; Rannou, P. Processible Conjugated Polymers: from Organic Semiconductors to Organic Metals and Superconductors. *Prog. Polym. Sci.* **2002**, *27*, 135−190.
(40) Athawale, A. A.; Kulkarni, M. V.; Chabukshwar, V. V. Studies on Chemically Synthesized Soluble Acrylic Acid Doped Polyaniline. *Mater. Chem. Phys.* **2002**, *73*, 106−110.
(41) Anitha, G.; Subramanian, E. Dopant Induced Specificity in Sensor Behaviour of Conducting Polyaniline Materials with Organic Solvents. *Sens. Actuators, B* **2003**, *92*, 49−59.
(42) Abthagir, P. S.; Saraswarhi, R. Junction Properties of Metal/Polypyrrole Schottky Barriers. *J. Appl. Polym. Sci.* **2001**, *81*, 2127−2135.
(43) Zhang, T.; Nix, M. B.; Yoo, B. Y.; Deshusses, M. A.; Myung, N. V. Electrochemically Functionalized Single-Walled Carbon Nanotube Gas Sensor. *Electroanalysis* **2006**, *18*, 1153−1158.
(44) Long, Y.; Chen, Z.; Zhang, X.; Zhang, J.; Liu, Z. Synthesis and Electrical Properties of Carbon Nanotube Polyaniline Composites. *Appl. Phys. Lett.* **2004**, *85*, 1796−1798.
(45) Bo, X. Z.; Tassi, N. G.; Lee, C. Y.; Strano, M. S.; Nuckolls, C.; Blanchet, G. B. Pentacene-Carbon Nanotubes: Semiconducting Assemblies for Thin-Film Transistor Applications. *Appl. Phys. Lett.* **2005**, *87* (203510), 1−3.
(46) Horowitz, G. Organic Field-Effect Transistors. *Adv. Mater.* **1998**, *10*, 365−377.
(47) Shklovskii, B. I. Hopping Conduction in Lightly Doped Semiconductors. *Sov. Phys. Semicond.* **1973**, *6*, 1053−1075.
(48) Brown, A. R.; Leeuw, D. M.; Havinga, E. E.; Pomp, A. A Universal Relation Between Conductivity and Field-Effect Mobility in Doped Amorphous Organic Semiconductors. *Synth. Met.* **1994**, *68*, 65−70.
(49) Hennrich, F.; Chan, C.; Moore, V.; Rolandi, M.; O'Connell, M. In *Carbon Nanotubes Properties and Applications*; O'Connell, M. J., Eds.; CRC Press: Boca Raton, FL, 2006; p 9.